

Field-grown soybean shows genotypic variation in physiological and seed composition responses to heat stress during seed development

Anna C. Ortiz^a, Ive De Smet^b, Rosangela Sozzani^c, Anna M. Locke^{a,d,*}

^a USDA-ARS Soybean and Nitrogen Fixation Research Unit, Rm. 4112 Williams Hall, 101 Derieux Place, Raleigh, NC, USA

^b VIB-UGent Center for Plant Systems Biology, Gent, Belgium

^c Department of Plant and Microbial Biology, North Carolina State University, Raleigh, NC, USA

^d Department of Crop and Soil Sciences, North Carolina State University, Raleigh, NC, USA

ARTICLE INFO

Keywords:

Photosynthesis

V_{cmax}

Respiration

Yield

Seed composition

ABSTRACT

An average temperature increase between 2.6 and 4.8 °C, along with more frequent extreme temperatures, will challenge crop productivity by the end of the century. To investigate genotypic variation in soybean response to elevated temperature, six soybean (*Glycine max*) genotypes were subjected to elevated air temperature of +4.5 °C above ambient for 28 days in open-top field chambers. Gas exchange and chlorophyll fluorescence were measured before and during heating and yield as well as seed composition were evaluated at maturity. Results show that long-term elevated air temperature increased nighttime respiration, increased the maximum velocity of carboxylation by Rubisco, impacted seed protein concentration, and reduced seed oil concentration across genotypes. The genotypes in this study varied in temperature responses for photosynthetic CO₂ assimilation, stomatal conductance, photosystem II operating efficiency, quantum efficiency of CO₂ assimilation, and seed protein concentration at maturity. These diverse responses among genotypes to elevated air temperature during seed development in the field, reveal the potential for soybean heat tolerance to be improved through breeding and underlines the importance of identifying efficient selection strategies for stress-tolerant crops.

1. Introduction

As a part of climate change, atmospheric temperatures are projected to increase worldwide at an average rate of 0.3 °C per decade, with a likely +1.5 °C rise in the next 20 years, corresponding to projections under the most severe climate models (Collins et al., 2013; Lee et al., 2021). In the United States, heat waves surpassing the optimum temperatures for crops are expected to increase in frequency, particularly in regions with high agricultural productivity (Gornall et al., 2010; Hatfield et al., 2011; Herring et al., 2016; Liang et al., 2017). The highest of the projected global mean temperature scenarios for the end of the century, RCP8.5, predicts an average temperature increase of 2.6–4.8 °C above current conditions (Collins et al., 2013). In addition, work by Zhao et al. (2017) predicts a yield reduction of 11.6% under RCP8.5 for soybean (*Glycine max*). Modeling predicts that a temperature change of

even 1.8–2.4 °C will stall soybean yield gains by mid-century (Iizumi et al., 2017). Yield reductions have been observed in elevated temperature field studies that have exposed soybean to short-term heat waves (Hatfield and Dold, 2019; Siebers et al., 2015; Thomey et al., 2019) as well as season-long warming (Ruiz-Vera et al., 2013). Soybean is responsible for 65% of protein feed globally (FAO, 2002) with over 82 million acres of soybean harvested in the United States in 2020 (United States Department of Agriculture, 2020). Improving soybean heat tolerance is vital for food security and identifying and harnessing genetic variation for heat stress response could play an important role in crop improvement.

In vitro and pot studies have found genotypic variation in soybean temperature response for seedling growth (Alsajri et al., 2019), seed composition (Alsajri et al., 2020; Chebroly et al., 2016; Nakagawa et al., 2020; Pipolo et al., 2004), photosynthetic responses (Herritt and

Abbreviations: A_n , net photosynthetic rate; AT, ambient temperature; ET, elevated temperature; g_s , stomatal conductance to water vapor; F_v/F_m , maximum quantum efficiency of PSII; F_v/F_m , quantum efficiency of PSII in the light; iWUE, intrinsic water use efficiency; J_{max} , maximum rate of linear electron transport through PSII; NPQ, nonphotochemical quenching; R_n , nighttime leaf respiration; R_d , mitochondrial respiration; T_{leaf} , leaf temperature; V_{cmax} , maximum rate of carboxylation of RuBP; VPD, vapor pressure deficit; Φ_{CO_2} , quantum efficiency of CO₂; Φ_{PSII} , quantum efficiency of PSII.

* Corresponding author at: USDA-ARS Soybean and Nitrogen Fixation Research Unit, Rm. 4112 Williams Hall, 101 Derieux Place, Raleigh, NC, USA.

E-mail address: Anna.Locke@usda.gov (A.M. Locke).

<https://doi.org/10.1016/j.envexpbot.2021.104768>

Received 18 August 2021; Received in revised form 14 December 2021; Accepted 26 December 2021

Available online 29 December 2021

0098-8472/Published by Elsevier B.V. This is an open access article under the CC BY license (<http://creativecommons.org/licenses/by/4.0/>).

Fritschi, 2020; Kumangai and Sameshima, 2014), and reproductive development (Kumangai and Sameshima, 2014; Salem et al., 2007). *In situ* studies enable the evaluation of temperature responses for crop canopies in open-air conditions with unbound root systems. To date, these studies have been restricted to a single genotype at a time (Rosenthal et al., 2014; Ruiz-Vera et al., 2013; Siebers et al., 2015; Thomey et al., 2019) or relied on historic data rather than experimentally controlled comparisons (Zheng et al., 2009). Multi-genotype field experiments are needed to evaluate genotypic variation in field conditions to support germplasm improvement.

This study tested the hypothesis that soybean will have genotypic variation for long-term heat stress responses in the field. This was tested by growing six soybean genotypes at + 4.5 °C elevated air temperature in the field during seed development, which occurs during what is typically the hottest period of the growing season. Air within open-top field plots was heated for four weeks during the seed development for maturity group III and IV genotypes in the absence of soil moisture limitation to identify responses that vary among genotypes under temperatures similar to the RCP8.5 projections for the end of the century (Collins et al., 2013).

2. Materials and methods

2.1. Site description and experimental design

Eight open-top field chambers of 9 m by 3 m, previously described by Qiu et al. (2018), were built at the Lake Wheeler Road Field Laboratory, in Raleigh, NC, USA. Each plot had two parallel, bi-layer 9 m plastic walls, perforated on the interior layer. At the center of the walls, the plastic connected to fan boxes which distributed heated air along the entire length of the plot through the perforations in the bi-layer plastic. The fan boxes attached to heated plots housed electrical resistance heating elements. In the split-plot design, an elevated temperature (ET) treatment was applied to four randomly selected plots. Untreated plots were only exposed to ambient temperatures (AT) with fan boxes distributing unheated air through the plots. Each plot was divided into six 3 m long subplots with two rows at 38 cm spacing. One of six soybean lines was randomly assigned to each subplot. The seeds were planted at a density of 20 seeds per meter and thinned to 12 plants per meter after emergence. Publicly released cultivars and advanced breeding lines were selected for favorable yield and/or seed composition traits. Wyandot-HP-47, Wyandot and Hipro1 were in maturity group III, and DBHIF 62-1, DBHIF 62-2 and N19-0346 were in maturity group IV.

Soils were fertilized according to soil quality tests, with 22 kg ha⁻¹ of NH₄NO₃ and 100.8 kg ha⁻¹ of K₂O prior to planting. Seeds were inoculated by spraying a suspension of 70 g N-Dure *Bradyrhizobium japonicum* inoculant (Verdesian, Cary, NC, USA) per 22.7 kg water after planting to ensure nodulation and atmospheric N₂ fixation.

The heat treatment lasted four weeks from August 17th to September 14th 2020, as maturity group III plants entered developmental stage R5 and maturity group IV plants were in R4, and heating ended when maturity group III plants reached R7 and maturity group IV were in R6, at which time leaf senescence had begun. Irrigation was applied through a drip line four days a week to maintain soils as close to field capacity as possible, as observed by sensor data (~0.28 m³ m⁻³), to focus the experiment on direct heat responses rather than indirect responses that would result from soil moisture limitation.

2.2. Physiological measurements

Leaf gas exchange and chlorophyll *a* fluorescence were measured with a LI-6800 photosynthesis system equipped with a leaf chamber fluorometer (6800-01 A, LI-COR Biosciences, Lincoln, NE, USA) to evaluate short-term physiological responses to elevated temperature. All gas exchange and fluorescence measurements were taken from an uppermost fully expanded leaf's middle leaflet. Dark-adapted chlorophyll

fluorescence (F_v/F_m , or the maximum quantum efficiency of photosystem II [PSII]) and respiration (R) were measured four hours after last light the night before treatment onset (day 0) and seven days into heating (day 7). Light-adapted chlorophyll fluorescence and gas exchange parameters were measured at midday on day 0 before temperature elevation began at 4:30 pm, and then repeated at midday 24 h (day 1) and 48 h (day 2) later. The physiological parameters measured at midday include net photosynthetic rate (A_n), stomatal conductance (g_s), the operating efficiency of PSII (F_v'/F_m'), PSII quantum efficiency (Φ PSII), and non-photochemical quenching (NPQ). Intrinsic water use efficiency (iWUE) was calculated from A_n and g_s . Light intensity, [CO₂], and air temperature inside the measurement chamber were set to match ambient conditions in the plots. Leaf temperature (T_{leaf}) and leaf-to-air vapor pressure deficit (VPD) measured inside the LI-6800 chamber during midday measurements are also reported.

Photosynthetic intercellular CO₂ response (A/C_i) curves were measured for all sub-plots. Replicates were blocked into four groups so that one replicate for each genotype-treatment combination was measured on each of four consecutive days, beginning seven days after heating. Before sunrise, the uppermost fully expanded leaves were excised at the base of the petiole and immediately placed in de-ionized water; the petioles were re-cut under water upon return to the lab to remove embolized vessels. Leaves were acclimated to actinic light for 30 min before measuring. The middle leaflet was clamped into a LI-6800 for measurement, and A_n and g_s were permitted to reach steady state. Gas exchange was measured in under 12 different CO₂ concentrations: 300, 200, 100, 50, 400, 400, 600, 800, 1000, 1200, 1500, 2000 μmol mol⁻¹. Light and temperature settings were based on average midday light intensity (1800 μmol m⁻² s⁻¹) and average treatment temperatures (32 °C and 36 °C for AT and ET, respectively) as recorded by canopy air sensors. The maximum rate of carboxylation by Rubisco (V_{cmax}), maximum rate of electron transport (J_{max}), and respiration in the light (R_d) were calculated from fitted simultaneous estimation based on the Farquhar, von Caemmerer, and Berry model (1980) and Dubois et al. (2007). K_c , K_o and Γ^* were calculated using the Michaelis-Menten constants for Rubisco O₂ and CO₂, measured using transgenic tobacco (Sharkey et al., 2007).

Daytime survey measurements of nonphotochemical quenching (NPQ) were calculated by pairing mean nighttime measurements from each plot following Eq. (1).

$$NPQ = \frac{(F_m - F_m')}{F_m'} \quad (1)$$

Where F_m is the nighttime maximal fluorescence and F_m' is light adapted maximal fluorescence as measured by the LI-6800.

2.3. Yield and seed composition

When plots reached maturity, all shoots were clipped at soil level and mechanically threshed. Seeds were weighed to determine yield for each subplot. Homogenous, whole-seed subsamples from each subplot were analyzed with near infrared spectroscopy (NIR) (DA 7250, Perten Instruments, Springfield, IL, USA) to measure protein and oil concentration. The calibration equation was created with thousands of seed samples of known oil and protein seed composition, processed with typical chemical protocols. Protein and oil concentrations were normalized to 13% moisture content.

2.4. Sensor network

Air temperature and relative humidity sensors (RXW-THC-900, Onset, Bourne, MA, USA) were installed in the center of each plot, 1 m above ground, just above the top of the crop canopy. Plot-level vapor pressure deficit (VPD) was calculated from these air temperature and relative humidity data. Soil moisture, electrical conductivity, and

temperature HOBO sensors (RXW-T12-900, Onset, Bourne, MA, USA) were installed at 10 and 40 cm depths at the center of each of the Wyandot genotype subplots. All sensor data was logged in 15-minute intervals.

2.5. Statistical analyses

All statistical analyses were conducted in R version 3.6.3. All data were fitted to the model(s) described below, and when the residuals for a variable were not normally distributed, it was transformed using the Box-Cox transformation or the Tukey Ladder of Powers with R packages MASS and rcompanion (Venables and Ripley, 2002; Mangiafico, 2016) (Table S1). Variables that did not require transformation included R , V_{cmax} , yield, seed protein concentration, and seed oil concentration. Residuals from the linear model for F_v/F_m and ΦPSII were not normally distributed even after transformation; therefore, the non-parametric Wilcoxon-rank sum test was used to test for differences between treatments and genotypes. All other variables were analyzed using linear mixed models described below, using lmer and lmerTest packages in R (Bates et al., 2015; Kuznetsova et al., 2017; R Core Team, 2019).

Measurements from day 0 (before heating) were used as a covariate for midday and nighttime gas exchange and chlorophyll fluorescence measurements. For midday measurements, date, treatment, and genotype were used as fixed effects, and plot number was a random intercept. Treatment comparisons within date were performed with the least-square means test from the lmerTest package. For nighttime measurements and variables derived from A/C_i data, treatment and genotype were fixed effects and block was a random intercept to account for the different days on which A/C_i responses was measured. Yield and seed composition data were analyzed with genotype and treatment as a fixed effect, and plot number was a random intercept. Three-way ANOVA and least square means from the mixed models were used to determine simple main effects and pairwise comparisons of genotype by treatment per day of measurement. These tests were performed in the lmerTest package. Pearson's correlation values were calculated for z-scores. All significant p -values from pairwise comparisons for gas exchange, nighttime respiration, V_{cmax} , J_{max} , yield and seed composition are presented in the Supplementary Materials (Table S2).

To reduce type II error when testing hypotheses with highly variable field data, α was selected to minimize the average of both type I and type II errors for each test (Mudge et al., 2012). Error rates were calculated over a range of power values from 0.1 to 0.9 with a Cohen's f corresponding to a medium effect size (Cohen, 1988) using the wp.kanova function from the WebPower package (Mudge et al., 2012; Zhang and Mai, 2018). This strategy yielded $\alpha = 0.17$ for gas exchange and chlorophyll fluorescence data and $\alpha = 0.16$ for harvest data. For pairwise comparisons within main effects, raw p -values were adjusted using the

Benjamini and Hochberg correction (Benjamini and Hochberg, 1995) and tested with $\alpha = 0.32$, which was determined as described above. For correlation tests, the same strategy yielded $\alpha = 0.14$ for a moderate effect size.

3. Results

3.1. Air temperature elevation achieved in open-air field plots

Mean air temperature difference between AT and ET plots was 4.5 °C from August 17th through September 14th. Mean canopy air temperature was 26 °C in AT and 30.5 °C in ET, with average day/night temperatures of 26.7/24.9 °C in AT and 31/29.9 °C in ET (Fig. 1). Relative humidity in ET plots was 18% lower than AT (66.2% and 85.3%, respectively) during the 4-week heating period. Average VPD in the plots was 0.65 kPa in AT and 1.6 kPa in ET plots. Ambient temperatures dropped approximately 4 °C, 13 days into heating. This change reduced both AT and ET averages for four days. The average solar noon temperatures in ET plots (22 °C) during this period were also lower than the warmest AT temperatures recorded during the treatment period (23 °C). An additional dip in nighttime temperatures 20 days into heating dropped AT to 23 °C and ET to 30 °C, when a few days before, these had been 28 °C and 32 °C, respectively.

Mean soil temperature was 2 °C higher in ET plots (Table 1). The mean difference in volumetric water content (VWC) between ET and AT plots at 10 cm and 40 cm depth was 0.01 m³m⁻³ (Table 1; Fig. 2), indicating that irrigation sufficiently compensated for the greater evapotranspiration in elevated temperature plots.

3.2. Leaf-level responses

3.2.1. A/C_i -derived responses

Photosynthetic responses were measured across a range of CO₂ concentrations from 50 to 2000 $\mu\text{mol mol}^{-1}$ to calculate biochemical limitations to photosynthesis for AT and ET plants. Here, only the

Table 1

Mean and standard deviation (Sd) for soil VWC and temperature by treatment and soil depth, ± 2 Sd, where AT and ET are ambient and elevated temperature treatments.

Treatment	Depth (cm)	Mean soil VWC (m ³ m ⁻³)	Mean soil temperature (°C)	Sd VWC (m ³ m ⁻³)	Sd soil temperature (°C)
AT	10	0.295	24.3	0.030	1.31
AT	40	0.312	24.7	0.030	0.71
ET	10	0.307	26.3	0.023	1.29
ET	40	0.299	26.2	0.011	0.91

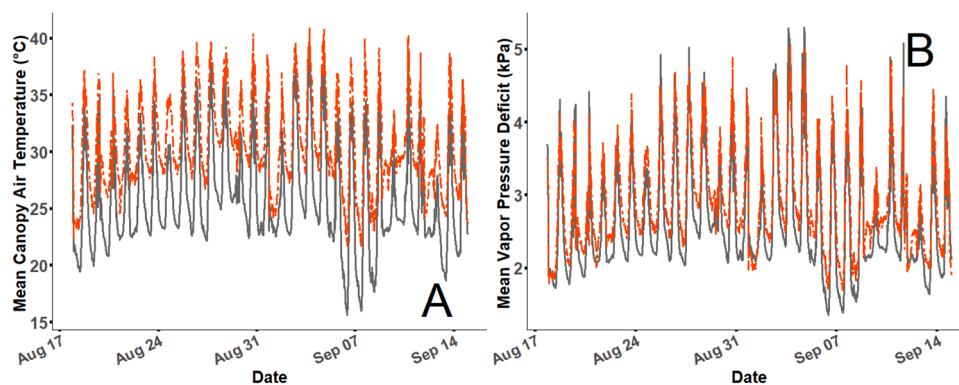


Fig. 1. A) Mean canopy air temperature and B) VPD measured within AT and ET plots during the treatment period, when plants were in R5-R7 developmental stages. Solid gray lines are measurements from AT plots, and orange dashed lines are measurements from ET plots. Sensors were mounted in the center of each plot, and temperature and relative humidity values were recorded every 15 min.

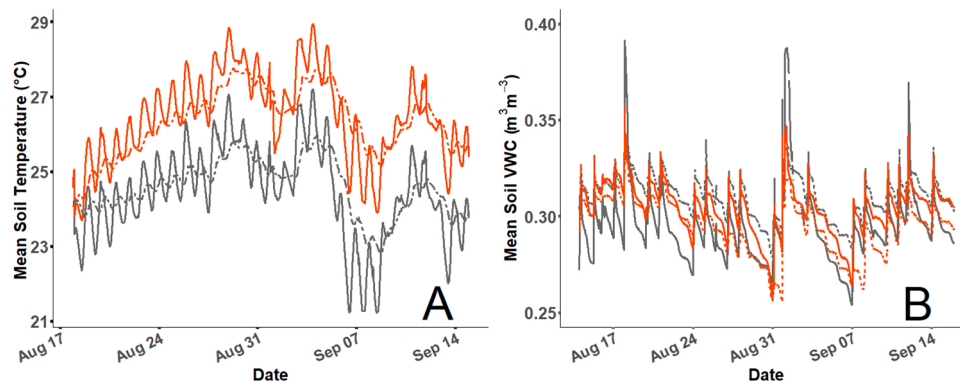


Fig. 2. A) Mean soil temperatures and B) and volumetric water content (VWC) at 10 cm and 40 cm soil depth in AT (grey) and ET (orange) plots. Solid lines are 10 cm depth measurements, and dashed lines are 40 cm depth measurements. The sensors were installed at the specified depths in the center of each Wyandot-47 sub-plot when plants were at the VC developmental stage, values were logged every 15 min.

genotype factor significantly affected J_{max} and R_d ($p = 0.02$ and $p = 0.0034$, Table 2). Non-transformed mean values for V_{cmax} , J_{max} and R_d are presented in Table 3. V_{cmax} was significantly affected by both temperature and genotype ($p < 0.01$, Table 2). V_{cmax} was higher at ET for DBHIF 62-1, DBHIF 62-2 and NI9-0346 (Table 3). There was no significant genotype by treatment effect for the A/C_i -derived parameters.

3.2.2. Nighttime measurements

Temperature significantly increased R by an average of 32% across genotypes (Table 3). The ET vs AT pairwise comparison was significant for DBHIF 62-2 and Wyandot genotypes. For F_v/F_m' , no significant differences between treatments or genotypes were found (Fig. 3). Only the Wyandot genotype had significantly different F_v/F_m' in ET plots (Table 4). Non-transformed mean values for nighttime respiration and maximum quantum efficiency in of PSII are presented in Table 3.

3.2.3. Midday measurements

Gas exchange and leaf chlorophyll fluorescence were measured at midday, when photosynthesis typically peaks, on day 1 and 2 of heating. Measurements taken before heating (day 0) were used as a covariate in the analysis. Air temperature was controlled inside the LI-6800 sample chamber during measurements to ensure that measurement conditions matched atmospheric conditions as closely as possible. Mean A_n , g_s , F_v'/F_m' and ΦCO_2 (statistically significant midday survey measurement variables) of non-transformed data per genotype, treatment and measurement day are presented in Table 5. Treatment did not significantly affect A_n . Genotype significantly affected A_n ($p = 0.01$), and the date by treatment interaction ($p = 0.09$) as well as the genotype by treatment interaction ($p = 0.07$) were significant (Table 6). A_n in DBHIF 62-1 was higher in ET at day 1 but not significantly different on day 2 (Table 7). DBHIF 62-2 had significantly higher A_n in ET than in AT, on day 2 ($p = 0.05$, Table 7, Table S1). Hipro1 had significantly lower A_n in ET plots than in AT plots two days into heating ($p = 0.09$, Table S1, Table 7).

Leaf temperature, measured inside the LI-6800 sample chamber while air temperature was controlled as in the plot treatment, was

Table 2

p-values from ANOVA for R, V_{cmax} , J_{max} , and R_d measured on Day 7. T indicates the fixed effect of the temperature treatment (ET vs. AT), G indicates the fixed effect of genotype, and T x G indicates the interaction between temperature and genotype.

	V_{cmax}	J_{max}	R_d
T	0.008*	0.8	0.96
G	0.0009*	0.02*	0.0034*
T x G	0.39	0.88	0.35

affected by date, treatment, and date by treatment interactions (Table 6). In addition, leaf temperatures were on average 12% higher for all genotypes on day 1 and 16% higher for all genotypes on day 2 (Table 7).

Stomatal conductance (g_s) was significantly affected by genotype ($p = 0.06$), but leaf temperature was not (Table 6). Interactions between date and treatment, date and genotype, and treatment and genotype were also significant (Table 6). On average, g_s decreased - 7.6% at ET two days into heating (Table 7). Only the main effect of date was significant for iWUE; with a significant interaction between date and genotype (Table 6).

The maximum quantum efficiency of photosystem II (F_v'/F_m') did not have significant main effects, but there were significant interactions between date and treatment, date and genotype, and treatment and genotype (Table 6). On day 2, F_v'/F_m' was significantly different between AT and ET for Wyandot HP-47.

Only the genotype effect was significant for NPQ (Table 6). The quantum efficiency of PSII ($\Phi PSII$) had significantly different values only on day 1 for all genotypes except NI9-0346 and Wyandot HP-47 (Table 4).

3.3. Harvest responses: yield and seed composition

At maturity, all plants were harvested, and seed yield and seed composition were evaluated for all genotypes and treatments. Genotype significantly affected yield ($p = 0.04$, Table 8). Treatment and genotype by treatment effects were not significant. Both protein and oil concentration were significantly affected by treatment and genotype (Table 8), and the treatment by genotype interaction was significant only for protein concentration. All genotypes had significantly lower oil concentration in ET plots (Table 9 and Table S2).

3.4. Multivariate analyses

Correlation coefficients highlight the negative relationship between leaf temperature and A_n , g_s , F_v'/F_m' , J_{max} , and R, similar to the responses of these variables to leaf temperature observed in the previous analyses. In addition, yield was negatively correlated with g_s , F_v'/F_m' , and R_d and positively correlated with NPQ (Table 10). Seed protein concentration was positively correlated with A_n and F_v'/F_m' and negatively correlated with R and seed oil concentration.

4. Discussion

This study was conducted to evaluate the responses of soybean genotypic variability during long-term elevated air temperature. The findings reveal variation among genotypes in short-term elevated

Table 3

Mean values of R , F_v/F_m , V_{cmax} , J_{max} , and R_d for each combination of genotype and treatment, and percent change for ET compared to AT. Asterisks indicate significant changes between AT and ET.

Genotype	R ($\mu\text{mol CO}_2 \text{ m}^{-2} \text{ s}^{-1}$)			F_v/F_m			V_{cmax} ($\mu\text{mol m}^{-2} \text{ s}^{-1}$)			J_{max} ($\mu\text{mol m}^{-2} \text{ s}^{-1}$)			R_d ($\mu\text{mol CO}_2 \text{ m}^{-2} \text{ s}^{-1}$)		
	AT	ET	% change	AT	ET	% change	AT	ET	% change	AT	ET	% change	AT	ET	% change
DBHIF 62-1	1.75	1.79	2.30	0.831	0.849	2.16	275.76	377.83	37.01*	332.92	313.77	-5.75	3.98	2.99	-24.71
DBHIF 62-2	1.52	2.29	51.0*	0.852	0.853	0.11	261.90	339.63	29.68*	337.54	325.06	-3.70	4.52	4.69	3.81
Hipro1	1.76	2.14	21.70	0.851	0.852	0.21	264.68	301.88	14.06	315.36	305.72	-3.06	5.76	4.82	-16.24
NI9-0346	1.44	2.02	41.30	0.830	0.846	1.88	305.11	450.31	47.59*	330.36	356.17	7.81	3.23	2.57	-20.41
Wyandot	1.37	2.09	51.8*	0.846	0.851	0.56*	221.04	285.07	28.96	264.79	302.85	14.37	5.07	7.88	55.32
Wyandot HP-47	1.81	2.26	24.90	0.853	0.846	-0.78	196.32	187.59	-4.45	263.86	245.54	-6.94	3.95	3.96	0.25
Average	1.61	2.10	22.55	0.844	0.850	0.69	257.13	323.72	25.48	307.47	308.19	0.45	4.42	4.49	-0.32

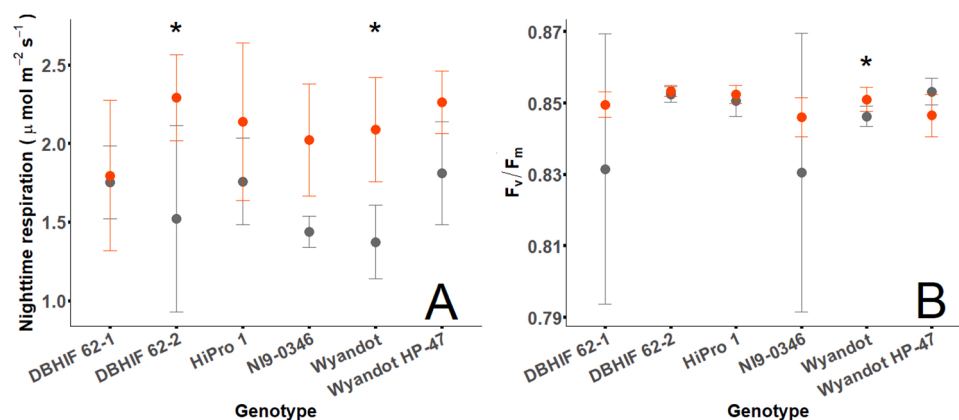


Fig. 3. Means and standard deviations for A) nighttime respiration and B) F_v/F_m seven days into heating. Grey dots and error bars are AT, and orange dots and error bars are ET. Asterisks indicate significant differences between treatments for a genotype.

Table 4

p-values from Wilcoxon-rank sum test for differences between ET and AT values for each genotype for midday measurements of ΦPSII on Day 1 and nighttime measurements of F_v/F_m on Day 7.

Genotype	Midday- Day 1 ΦPSII	Nighttime- Day 7 F_v/F_m
DBHIF 62-1	0.114*	1
DBHIF 62-2	0.028*	0.625
Hipro1	0.114*	0.625
NI9-0346	0.486	0.875
Wyandot	0.057*	0.125*
Wyandot HP-47	0.68	0.375

temperature responses as well as seed composition after long-term seed development at ET.

4.1. Genetic variability in leaf level responses

The elevated air temperature treatment in this study increased air temperatures at canopy height by 4.5 °C over ambient, reduced relative humidity by 18%, and elevated plot VPD by 1 kPa for 28 days during reproductive development in the field. Although higher VPD increases transpiration demand, irrigation was applied to minimize the soil moisture differential between treatments. Therefore, this experiment tested the direct effects of a warmer atmosphere rather than indirect temperature effects via progressive soil moisture limitation.

Heating the air, rather than the leaf surface (e.g., by infrared heaters), meant that plant biochemical responses to the elevated temperature treatment could vary among genotypes depending on genotypic differences in latent heat exchange via stomatal conductance. Although g_s responses to air temperature varied among genotypes, no genotypic differences were observed for leaf temperature measured in the LI-6800 leaf chamber, while air temperature was controlled. Stomatal conductance responses to temperature varied among genotypes and between measurement days. All the genotypes had increased g_s after one day of heating, except for Wyandot HP-47, but only two genotypes, DBHIF 62-2 and NI9-0346 increased g_s after two days, making these less sensitive to heat stress (Table 7). Although biochemical responses are more difficult to interpret in the context of air temperature than in relation to leaf temperature (Jagadish et al., 2021), plant physical traits and stomatal responses to atmospheric warming will be an integral component of crop response and potential adaptation to global warming (Buckley, 2019; Lin et al., 2017).

Only three physiological parameters measured in this study, V_{cmax} , R , and oil, responded to elevated temperature without a treatment by genotype interaction. Oil concentration consistently declined at ET and had a negative correlation with protein, as is commonly observed across soybean datasets (Lee et al., 2019). Soybean's market value partly hinges on this component, and a decrease could reduce soybean's value.

For A_n and F_v'/F_m' , elevated temperature had different effects among genotypes and between measurement days (Table 7, Table S2). Prior single-genotype studies have found soybean A_n to generally be reduced by elevated temperature and heat waves (Ruiz-Vera et al., 2013; Siebers

Table 5

Mean values for A_n , g_s , F_v'/F_m' , and ΦCO_2 measurements on day 1 and day 2 of the elevated temperature treatment, grouped by treatment (AT or ET) and genotype. These values were transformed for statistical analysis as described in Table S1.

Genotype	A_n ($\mu\text{mol CO}_2 \text{ m}^{-2} \text{ s}^{-1}$)				g_s ($\text{mmol H}_2\text{O m}^{-2} \text{ s}^{-1}$)				F_v'/F_m'				ΦCO_2			
	Day1		Day2		Day1		Day2		Day1		Day2		Day1		Day2	
	AT	ET	AT	ET	AT	ET	AT	ET	AT	ET	AT	ET	AT	ET	AT	ET
DBHIF 62-1	41.75	46.35	37.44	36.54	1.12	1.18	0.90	0.78	0.62	0.63	0.61	0.59	0.03	0.03	0.03	0.03
DBHIF 62-2	33.53	43.16	36.12	45.29	0.57	0.97	0.76	1.04	0.57	0.62	0.60	0.63	0.02	0.03	0.02	0.03
HiPro 1	42.39	44.81	43.97	37.68	0.89	0.75	1.17	0.78	0.63	0.64	0.63	0.59	0.03	0.03	0.03	0.03
NI9-0346	41.25	41.31	37.25	34.75	0.89	1.01	0.98	0.94	0.62	0.62	0.63	0.61	0.03	0.03	0.03	0.02
Wyandot	35.00	40.24	38.37	32.58	0.95	0.98	1.09	0.83	0.61	0.61	0.65	0.60	0.02	0.03	0.03	0.02
Wyandot HP-47	27.12	30.46	38.83	34.58	0.55	0.58	0.92	0.85	0.57	0.55	0.66	0.59	0.02	0.02	0.03	0.02
Average	36.84	41.06	37.27	36.9	0.83	0.91	0.91	0.87	0.60	0.61	0.63	0.61	0.03	0.03	0.03	0.03

Table 6

P-values from ANOVA for A_n , T_{leaf} , g_s , F_v'/F_m' , NPQ, and iWUE measured at mid-day on Day 1 and Day 2 of the ET treatment as well as R measured at nighttime on Day 7. T indicates the fixed effect of the temperature treatment (ET vs. AT), G indicates the fixed effect of genotype, and D indicates the day effect (day 1 vs day 2) for parameters measured on two days.

	Midday						Nighttime
	A_n	T_{leaf}	g_s	iWUE	F_v'/F_m'	NPQ	
D0	0.78	0.85	0.76	0.87	0.57	0.79	0.08
D	0.22	0.02*	0.6	0.02*	0.45	0.22	
T	0.6	0.02*	0.99	0.93	0.48	0.92	0.01*
G	0.01*	0.33	0.06*	0.17	0.88	0.01*	0.17
D x T	0.09*	0.01*	0.07*	0.34	0.07*	0.18	
D x G	0.26	0.36	0.07*	0.10*	0.04*	0.27	
T x G	0.07*	0.21	0.03*	0.33	0.08*	0.27	0.21
D x T x G	0.86	0.91	0.59	0.84	0.93	0.86	

et al., 2015); although the effect varied somewhat among measurement days in both of these studies. In this study, A_n responded significantly for three specific genotypes. At day 1 of temperature elevation, A_n was higher in one out of six genotypes despite g_s not responding significantly for any genotype. At day 2, A_n was significantly lower for HiPro1 at ET (Table 7). The shift in A_n response to ET between days may have resulted from higher V_{cmax} observed in ET paired with reduced F_v'/F_m' at day 2 (Table 7). DBHIF 62-2 was the only genotype with a large increase in A_n (25.4%) under ET on day 2 (Table 7). Although g_s was reduced by direct canopy heating in the field (Ruiz-Vera et al., 2013; Siebers et al., 2015), the g_s responses observed here from air warming were not consistent. This finding also differs from the consistent g_s increase at warmer air temperatures in growth chambers that was observed by Herritt and Frittschi (2020).

Another difference between this and prior canopy warming experiments in the field is the timing and duration of temperature elevation. For example, Ruiz-Vera et al. (2013) applied a +3.5 °C throughout the entirety of the growing season and Siebers et al. (2015) applied a +6 °C heatwave for three days during four different developmental stages. Possible early-season acclimation to elevated temperature in this experiment might not have been captured by this study, which focused

Table 7

Percent change at ET compared to AT for A_n , T_{leaf} , g_s , F_v'/F_m' , NPQ, and iWUE measured at mid-day on day 1 and day 1 of ET treatment. Asterisks indicate significant changes between AT and ET.

Genotype	Day 1						Day 2					
	A_n	T_{leaf}	g_s	F_v'/F_m'	NPQ	iWUE	A_n	T_{leaf}	g_s	F_v'/F_m'	NPQ	iWUE
DBHIF 62-1	11.02*	11.82*	4.79	0.64	5.72	6.21	-2.42	15.39*	-13.41	-3.43	8.24	8.12
DBHIF 62-2	28.71	7.69	69.99	8.47	-19.56	-37.51	25.40*	12.74*	37.01	4.25	-18.42	-11.73
HiPro1	5.72	16.00*	-16.22	1.49	-17.78	11.83	-14.32*	21.81*	-33.54	—	—	26.62
NI9-0346	0.14	12.76*	13.48	-0.54	-107.56	-12.18	-6.71	14.97*	-3.69	-5.26	-106.25	3.94
Wyandot	14.97	13.02*	3.43	0.26	-5.99	-12.39	-15.11	19.16*	-23.92	-5.95	9.91	15.46
Wyandot HP-47	12.30	11.66*	5.62	-3.66	-1.54	-12.51	-10.95	15.97*	-8.12	-8.84*	31.43	-4.58
Average	12.14	12.16	13.52	1.11	-24.45	-9.42	-4.02	16.67	-7.61	-3.85	-15.02	6.31

on elevated temperature during the seed fill period only and included the beginning of leaf senescence. Conversely, the four-week duration of the treatment in this study may have allowed for acclimation to occur that would not have been observed in the prior short-term heatwave experiment.

Seed composition was affected by ET (Tables 8, 10). Oil concentration was the most consistent of all variables measured in this study: ET reduced oil concentration by a similar magnitude across all six genotypes. Although the effect of ET on protein was not significant for individual genotypes, the direction of change was positive in four genotypes (DBHIF 62-1, DBHIF 62-2, NI9-0346 and Wyandot) and negative in the other two. Yield was too highly variable to resolve temperature effects statistically, but it is important to note that trends for yield responses to ET were dissimilar in direction and magnitude across the six genotypes.

The maximum rate of carboxylation of ribulose-1, 5-biphosphate (RuBP) by carboxylase-oxygenase (Rubisco) activity (V_{cmax}) commonly limits photosynthetic carbon assimilation in non-stressed plants under ambient conditions (Bernacchi et al., 2009). Rosenthal et al. (2014) and Cen and Sage (2005) have shown that supra-optimum temperatures for plant growth do not limit V_{cmax} , and that high V_{cmax} at higher temperatures may shift the limitation to J_{max} at similar intercellular CO_2 concentrations. Above the temperature optimum, V_{cmax} increases, but Rubisco activity is limited as oxygenation increases and CO_2 solubility declines (Jordan and Ogren, 1984; Salvucci and Crafts-Brandner, 2004). As temperatures increase above the optimum, linear electron transport

Table 8

ANOVA table for mixed models comparing the effect of treatment and genotype on yield, protein, and oil concentration. p-values from ANOVA for yield, seed protein concentration, and seed oil concentration measured at maturity. T indicates the fixed effect of the temperature treatment (ET vs. AT) and G indicates the fixed effect of genotype.

	Yield	Protein	Oil
T	0.83	0.02*	<0.001*
G	0.04*	<0.001*	<0.001*
T x G	0.28	0.16*	0.76

Table 9

Mean values of yield, seed oil concentration, and seed protein concentration measured at maturity for each combination of genotype and treatment, and percent change for ET compared to AT. Asterisks indicate significant changes between AT and ET. Seed oil and protein concentrations are expressed on a 13% seed moisture basis.

Genotype	Yield (kg m ⁻²)			Oil (%)			Protein (%)		
	AT	ET	% change	AT	ET	% change	AT	ET	% change
DBHIF 62-1	0.77	0.74	-3.89	17.9	17.08	-5.02*	39.57	40.8	3.29
DBHIF 62-2	0.9	0.83	-7.77	17.96	17.31	-3.35*	39.28	40.43	3.06
HiPro 1	0.61	0.62	1.63	18.48	17.77	-3.80*	43.16	42.6	-1.16
N19-0346	0.866	0.66	-23.25	20.74	19.38	-6.31*	38.76	40.15	2.82
Wyandot	0.64	0.76	18.75	21.4	20.99	-2.33*	36.12	36.42	0.83
Wyandot HP-47	0.69	0.79	14.49	18.66	18.5	-3.22*	41.12	40.66	-0.97
Average	0.75	0.73	-0.01	19.19	18.51	-24.03	39.67	40.18	1.31

Table 10

Correlation coefficients for leaf gas exchange, chlorophyll a fluorescence, and harvest parameters measured in this experiment. Correlation coefficients were based on z-scores calculated across all genotypes and both treatments. Asterisks indicate significant correlation ($p \leq 0.14$).

	g_s	F_v'/F_m'	NPQ	T_{leaf}	$V_{c,max}$	J_{max}	R_d	R	Yield	Protein	Oil
A_n	0.81*	0.83*	-0.46*	-0.41*	0.33*	0.27*	-0.26*	-0.01	-0.09	0.26*	-0.19*
g_s		0.62*	-0.23*	-0.47*	0.24*	0.21*	-0.26*	-0.01	-0.19*	0.17	-0.17
F_v'/F_m'			-0.66*	-0.42*	0.15	0.13	-0.16	-0.01	-0.19*	0.29*	-0.04
NPQ				-0.04	-0.14	-0.01	0.06	0.03	0.20*	-0.16	-0.12
T_{leaf}					0.10	-0.27*	0.11	-0.34*	0.00	0.02	-0.13
$V_{c,max}$						0.57*	-0.48*	0.09	0.07	-0.12	0.06
J_{max}							-0.22*	0.19*	0.04	0.04	-0.07
R_d								-0.27*	-0.34*	0.09	0.02
R									0.16	-0.25*	0.19*
Yield										-0.18	-0.08
Protein											-0.61*

rate efficiency decreases, and RuBP regeneration, which is directly linked to J_{max} through PSII limits A_n (Farquhar et al., 1980). However, J_{max} was not affected by treatment after the first week of heating, and the lower ambient temperature that occurred during the heating event might have protected yield by preventing ET from exceeding the optimum.

Although supra-optimum temperatures would likely not limit $V_{c,max}$, and the main temperature effect was significant across genotypes in this study, the overall increase in $V_{c,max}$ was driven by larger, significant increases for three of the six genotypes. It is possible that the variation in $V_{c,max}$ responses observed here is related to genotypic variation in Rubisco activase (RCA) between genotypes or morphological differences affecting mesophyll conductance. The expression of Rubisco activase was shown to vary and correlate with seed yield across population of soybean landraces (Chao et al., 2014). Another potential source of genotypic variation in $V_{c,max}$ response is mesophyll conductance (g_m), which has been found to vary among 12–15 soybean genotypes in two separate studies (Bunce, 2016; Tomeo and Rosenthal, 2017). The temperature response of g_m also varied among three soybean genotypes in another study (Shrestha et al., 2019). Although increasing g_m with temperature may improve photosynthesis until J_{max} becomes limiting, the benefit of higher g_m could be offset by reduced stomatal conductance (Flexas et al., 2014), as was observed for Wyandot HP-47 at ET in this study.

Although this experiment was conducted at ambient atmospheric CO₂, which was approximately 415 ppm during the 2020 growing season, this value could increase to as high as 1000 ppm by the end of the century (Collins et al., 2013). Most directly, atmospheric CO₂ concentration at this level would increase intercellular CO₂ concentration beyond the saturation point of Rubisco, while $V_{c,max}$ and J_{max} are expected to acclimate to higher CO₂ concentration (Bernacchi et al., 2005; Rogers and Humphries, 2000). This could reduce the temperature effect observed here in all genotypes, even at more moderately elevated CO₂ concentration (Rosenthal et al., 2014). In the context of this study, if $V_{c,max}$ were to acclimate rapidly to a concomitant elevation in atmospheric CO₂ concentration, the increase in A_n observed here at day 1 might not occur.

Short-term dips in ambient temperature during the heating event shifted ET closer to optimum temperatures, partially ameliorating the impact of ET on yield and seed composition. Rapid recovery from heat waves has been observed following brief heat waves in soybean, wheat, and *Eucalyptus parramattensis* (Drake et al., 2018; Rashid et al., 2018; Siebers et al., 2015).

Nighttime respiration increases with temperature have been linked with yield loss in rice (Mohammed and Tarpley, 2009; Peng et al., 2004; Saitoh et al., 1998) and wheat (Tan et al., 2013). Although ET increased R in this study, yield may have been rescued by higher A_n observed in some genotypes, enabled by irrigation. In contrast with previous work (Siebers et al., 2015), ET increased R by an average of 32%, but the increase ranged from 2% to over 50% among genotypes. If higher R reduces yield in the absence of irrigation, this wide R response range could be harnessed to mitigate yield loss at higher temperatures.

4.2. Temperature sensibility and timing

The developmental timing of temperature elevation can affect its impact on yield and seed composition (Rotundo and Westgate, 2009; Siebers et al., 2015). Yield can be highly influenced by heat stress during flowering or pod development, when flowers and seeds may be aborted. Lesser effects of temperature on protein have been found in vitro when soybean is in seed filling stages than when temperature is increased during flowering and seed pod development (R1–R5) (Rotundo and Westgate, 2009). Similarly, chamber and in vitro studies by Xu et al. (2016) and Pipolo et al. (2004) found increased protein concentration when temperature exceeds 25–28 °C or 25–33 °C, respectively. In this study, seed protein concentration was dissimilar across genotypes and negative correlations with oil concentration were found. This negative correlation is commonly reported for soybean (Watanabe and Nagasawa, 1990; Li et al., 2014; Wijewardana et al., 2019). The reduction in seed oil concentration across genotypes in this field study contrasts starkly with prior chamber and in vitro studies, which found higher oil concentration at higher temperatures (Nakagawa et al., 2020; Chebroli et al., 2016; Pipolo et al., 2004). The explanation for the reduction in seed oil concentration observed here is not immediately clear, although

previous studies have found variability in fatty acid responses to high temperature. Linoleic and linolenic acids have been found to decline at higher temperatures, while oleic acid percentages increased at higher temperatures during seed fill (Carrera et al., 2011; Gibson and Mullen, 1996).

5. Conclusion

Our initial hypothesis, that soybean genotypes will vary in physiological and agronomic responses to elevated temperature, was supported by data from six soybean genotypes grown at 4.5 °C above ambient during seed development in open-air field plots. Photosynthesis and related parameters were affected differently among genotypes and between 1 and 2 days into heating. Elevated temperatures induced higher nighttime respiration rates, although yield was unaffected in the absence of water stress. Higher temperatures reduced oil concentration in all genotypes and affected seed protein differently among genotypes, which will greatly affect soybean's value to end users in future climate conditions. These findings indicate that genetic variability in existing soybean germplasm, even among existing cultivars and advanced breeding lines, could be harnessed to improve crop resiliency in a warmer future and highlight the importance of considering grain composition in abiotic stress studies. Future work in experimental field settings like the one presented here will be able to identify temperature tolerant soybean genotypes that can help adapt crops for future climate conditions.

Author Contributions

A.M.L., I.D.S., and R.S. conceived of the study and obtained funding. A.C.O. and A.M.L. conducted the experiment. A.C.O. conducted the data analyses and drafted the manuscript. A.C.O. and A.M.L. made most revisions to the manuscript. All authors reviewed, commented on, and approved the final version of the manuscript to be submitted.

CRedit authorship contribution statement

Anna C. Ortiz: Investigation, Formal analysis, Visualization, Writing – original draft, Writing – review & editing. **Ive De Smet:** Conceptualization, Funding acquisition, Writing – review & editing. **Rosangela Sozzani:** Conceptualization, Funding acquisition, Writing – review & editing. **Anna M. Locke:** Conceptualization, Funding acquisition, Writing – review & editing, Supervision.

Funding

This work was supported by the Foundation for Food and Agriculture Research [Grant no. CA18-SS-000000026], Benson Hill, BASF, the United Soybean Board [Grant no. 2020-152-0134], and the North Carolina Soybean Producers Association [Grant no. 20-122].

Declaration of Competing Interest

The authors declare the following financial interests/personal relationships which may be considered as potential competing interests: Anna M. Locke, Rosangela Sozzani, Ive De Smet reports financial support was provided by Foundation for Food and Agriculture Research. Anna M. Locke reports financial support was provided by United Soybean Board. Anna M. Locke, Rosangela Sozzani reports financial support was provided by North Carolina Soybean Producers Association. Anna M. Locke, Rosangela Sozzani reports financial support was provided by Benson Hill. Anna M. Locke reports financial support was provided by BASF.

Acknowledgements

The authors would like to thank Samuel Ray, Jeff Barton, Amanda Bailey, Pablo Rios, Kaleigh Smeltzer, and Walt Pursley for technical support in constructing and operating the heated plots. We thank Rouf Mian for generously providing the soybean seed used in this experiment.

Appendix A. Supporting information

Supplementary data associated with this article can be found in the online version at [doi:10.1016/j.envexpbot.2021.104768](https://doi.org/10.1016/j.envexpbot.2021.104768).

References

- Alsajri, F.A., Singh, B., Wijewardana, C., Irby, T., Gao, W., Reddy, K.R., 2019. Evaluating soybean cultivars for low- and high-temperature tolerance during the seedling growth stage. *Agronomy* 9 (13), 13. <https://doi.org/10.3390/agronomy9010013>.
- Alsajri, F.A., Wijewardana, C., Irby, J., Bellaloui, N., Krutz, L.J., Golden, B.S., Gao, W., Reddy, K.R., 2020. Developing functional relationships between temperature and soybean yield and seed quality. *Agron. J.* 112, 194–204. <https://doi.org/10.1002/agt2.20034>.
- Bates, D., Machler, M., Bolker, B., Walker, S., 2015. Fitting linear mixed-effects models using lme4. *J. Stat. Softw.* 67 (1), 1–48. <https://doi.org/10.18637/jss.v067.i01>.
- Benjamini, Y., Hochberg, Y., 1995. Controlling the false discovery rate: a practical and powerful approach to multiple testing. *J. R. Stat. Soc. Ser. B* 57, 289–300. <https://doi.org/10.1111/j.2517-6161.1995.tb02031.x>.
- Bernacchi, C., Morgan, P.B., Ort, D.R., Long, S.P., 2005. The growth of soybean under free air [CO₂] enrichment (FACE) stimulates photosynthesis while decreasing in vivo Rubisco capacity. *Planta* 2 (3), 434–446. <https://doi.org/10.1007/s00425-004-1320-8>.
- Bernacchi, C., Rosenthal, D., Pimentel, C., Long, S.P., Farquhar G.D., 2009. Modeling the temperature dependence of C3 photosynthesis (pp. 231–246). https://doi.org/10.1007/978-1-4020-9237-4_10.
- Buckley, T.N., 2019. How do stomata respond to water status? *New Phytol.* 224, 21–36. <https://doi.org/10.1111/nph.15899>.
- Bunce, J., 2016. Variation among soybean cultivars in mesophyll conductance and leaf water use efficiency. *Plants* 5, 44. <https://doi.org/10.3390/plants5040044>.
- Carrera, C., Martínez, M.J., Dardenelli, J., Balzarini, M., 2011. Environmental variation and correlation of seed components in nontransgenic soybeans: protein, oil, unsaturated fatty acids, tocopherols, and isoflavones. *Crop Sci.* 51, 51–809.
- Cen, Y.P., Sage, R.F., 2005. The regulation of rubisco activity in response to variation in temperature and atmospheric CO₂ partial pressure in sweet potato. *Plant Physiol.* 139 (2), 979–990.
- Chao, M., Yin, Z., Hao, D., Zhang, J., Song, H., Ning, A., Xu, X., Yu, D., 2014. Variation in Rubisco activase (RCAp) gene promoters and expression in soybean [Glycine max (L.) Merr]. *J. Exp. Bot.* 65 (1), 47–59. <https://doi.org/10.1093/jxb/ert346>.
- Chebrolo, K., Fritsch, F.B., Ye, S., Krishnan, H.B., Smith, J.R., Gillman, J.D., 2016. Impact of heat stress during seed development on soybean seed metabolome. *Metabolomics* 12, 28. <https://doi.org/10.1007/s11306-015-0941-1>.
- Cohen, J., 1988. *Statistical Power Analysis for the Social Sciences*, second ed. Lawrence Erlbaum Associates, Hillsdale, New Jersey.
- Collins, M., Knutti, R., Arblaster, J., Dufresne, J.-L., Fichefet, T., Friedlingstein, P., Gao, X., Gutowski, W.J., Johns, T., Krinner, G., Shongwe, M., Tebaldi, C., Weaver, A. J., Wehner, M., 2013. Long-term climate change: projections, commitments and irreversibility. In: Stocker, T.F., Qin, D., Plattner, G.-K., Tignor, M., Allen, S.K., Boschung, J., Nauels, A., Xia, Y., Bex, V., Midgley, P.M. (Eds.), *Climate Change 2013: The Physical Science Basis. Contribution of Working Group I to the Fifth Assessment Report of the Intergovernmental Panel on Climate Change*. Cambridge University Press, Cambridge, United Kingdom and New York, NY, USA.
- Drake, J., Tjoelker, M., Varhammaer, A., 2018. Trees tolerate an extreme heatwave via sustained transpirational cooling and increased leaf thermal tolerance. *Glob. Change Biol.* 24 (6), 2390–2402.
- Dubois, J.J.B., Fiscus, E.L., Booker, F.L., Flowers, M.D., Reid, C.D., 2007. Optimizing the statistical estimation of parameters of the Farquhar-von Caemmerer-Berry model of photosynthesis. *New Phytol.* 176, 402–414. <https://doi.org/10.1111/j.1469-8137.2007.02182.x>.
- FAO, 2002. Protein sources for the animal industry. FAO Expert Consultation and Workshop, Bangkok. 29 Apr.–3 May 2002. FAO, Rome.
- Farquhar, G.D., von Caemmerer, S., Berry, J.A., 1980. A biochemical model of photosynthetic CO₂ assimilation in leaves of C3 species. *Planta* 149, 78–90.
- Flexas, J., Diaz-Espejo, A., Cpnesa, M.A., Coopman, R.E., Douthe, C., Gago, J., Galmes, J., Medrano, H., Ribas-Carbo, M., Tomas, M., Niinemets, T.U., 2014. Mesophyll conductance to CO₂ and Rubisco as targets for improving intrinsic water use efficiency in C3 plants? *Plant. Cell Environ.* 39. <https://doi.org/10.1111/pce.12622>.
- Gibson, L.R., Mullen, R.E., 1996. Soybean seed composition under high day and night growth temperatures. *JOACS* 73, 733–737.
- Gornall, J., Betts, R., Burke, E., Clark, R., Camp, J., Willett, K., Wiltshire, A., 2010. Implications of climate change for agricultural productivity in the early twenty-first century. *Philos. Trans. R. Soc. Biol. Sci.* 365, 2973–2989.
- Hatfield, J., Dold, C., 2019. Water-use efficiency: advances and challenges in a changing climate. *Front. Plant Sci.* 10, 1–14. <https://doi.org/10.3389/fpls.2019.00103>.

- Hatfield, J.L., Boote, K.J., Kimball, B.A., Ziska, L.H., Izaurralde, R.C., Ort, D.R., Wolfe, D., 2011. Climate impacts on agriculture: implications for crop production. *Agron. J.* 103, 351–370.
- Herring, S.C., Hoell, A., Hoerling, M.P., Kossin, J.P., Schreck, C.J., Stott, P.A., 2016. Explaining extreme events of 2015 from climate perspective. *Bull. Am. Meteorol. Soc.* 97 (12), S1–S145.
- Herritt, M.T., Fritschi, F.B., 2020. Characterization of photosynthetic phenotypes and chloroplast ultrastructural changes of soybean (*Glycine max*) in responses to elevated air temperature. *Front. Plant Sci.* 11, 153.
- Iizumi, T., et al., 2017. Responses of crop yield growth to global temperature and socioeconomic changes. *Sci. Rep.* 7 (7800), 2017. <https://doi.org/10.1038/s41598-017-08214-4>.
- Jagadish, S.V.K., Way, D.A., Sharkey, T.D., 2021. Plant heat stress: concepts directing future research. *Plant Cell Environ.* 1–14. <https://doi.org/10.1111/pce.14050>.
- Jordan, D.B., Ogren, W.L., 1984. The CO₂/O₂ specificity of ribulose 1,5-bisphosphate carboxylase/oxygenase: dependence on ribulosebisphosphate concentration, pH and temperature. *Planta* 161 (4), 308–313. <https://doi.org/10.1007/BF00398720>.
- Kumangai, E., Sameshima, R., 2014. Genotypic differences in soybean yield responses to increasing temperature in a cool climate are related to maturity group. *Agric. For. Meteorol.* 198–199, 265–272.
- Kuznetsova, A., Brockhoff, P.B., Christensen, R.H.B., 2017. lmerTest package: tests in linear mixed effects models. *J. Stat. Softw.* 82 (13), 1–26. <https://doi.org/10.18637/jss.v082.i13>.
- Lee, J.-Y., J. Marotzke, G. Bala, L. Cao, S. Corti, J.P. Dunne, F. Engelbrecht, E. Fischer, J. C. Fyfe, C. Jones, A. Maycock, J. Mutemi, O. Ndiaye, S. Panickal, and T. Zhou: 2021, Future Global Climate: Scenario-Based Projections and Near-Term Information. In *Climate Change 2021: The Physical Science Basis. Contribution of Working Group I to the Sixth Assessment Report of the Intergovernmental Panel on Climate Change* [Masson-Delmotte, V., P. Zhai, A. Pirani, S.L. Connors, C. Péan, S. Berger, N. Caud, Y. Chen, L. Goldfarb, M.I. Gomis, M. Huang, K. Leitzell, E. Lonnoy, J.B.R. Matthews, T. K. Maycock, T. Waterfield, O. Yelekçi, R. Yu, and B. Zhou (eds.)]. Cambridge University Press. In Press.
- Lee, S., Van, K., Sung, M., Nelson, R., LaMantia, J., McHale, L.K., Mian, M., 2019. Genome-wide association study of seed protein, oil and amino acid contents in soybean from maturity groups I to IV. *Theor. Appl. Genet.* 132, 1639–1659. <https://doi.org/10.1007/s00122-019-03304-5>.
- Li, Y., Ming, D., Zhang, Q., Wang, G., Jin, J., Herbert, S., Liu, X., 2014. Planting date influences fresh pod yield and seed chemical compositions of vegetable soybean. *HortScience* 49 (11), 1376–1380. <https://doi.org/10.21273/hortsci.49.11.1376>.
- Liang, X.Z., Wu, Y., Chambers, R.G., Schmoldt, D.L., Gao, W., Liu, C., Liu, Y.A., Sun, C., Kennedy, J.A., 2017. Determining climate effects on US total agricultural productivity. *Proc. Natl. Acad. Sci. U.S.A.* 11 (12), 2285. <https://doi.org/10.1073/pnas.1615922114>.
- Lin, H., Chen, Y., Zhang, H., Fu, P., Fan, Z., 2017. Stronger cooling effects of transpiration and leaf physical traits of plants from a hot dry habitat than from a hot wet habitat. *Funct. Ecol.* 31, 2202–2221. <https://doi.org/10.1111/1365-2435.12923>.
- Mangiafico, S.S., 2016. Summary and Analysis of Extension Program Evaluation in R, version 1.18.7. [rcompanion.org/handbook/\(Pdf version: \(rcompanion.org/doc uments/RHandbookProgramEvaluation.pdf\)\)](https://rcompanion.org/handbook/(Pdf%20version%3A(rcompanion.org/doc%20uments/RHandbookProgramEvaluation.pdf))).
- Mohammed, A., Tarpley, L., 2009. Impact of high nighttime temperature on respiration, membrane stability, antioxidant capacity and yield of rice plants. *Crop Sci.* 49 (1), 313–332.
- Mudge, J.F., Baker, L.F., Edge, C.B., Houlahan, J.E., 2012. Setting an optimal α that minimizes errors in null hypothesis significance test. *PLoS One* 7 (2), e3273.
- Nakagawa, A.C.S., Ario, N., Tomita, Y., Tanka, S., Murayama, N., Mizuta, C., Iwaya-Inoue, M., Ishibashi, Y., 2020. High temperature during soybean seed development differentially alters lipid and protein metabolism. *Plant Prod. Sci.* 23 (4), 504–516.
- Peng, S., Huang, J., Sheehy, J.E., Laza, R.C., Visperas, R.M., Zhong, X., Centeno, G.S., Khush, G.S., Cassman, K.G., 2004. Rice yields decline with higher night temperature from global warming. *Proc. Natl. Acad. Sci. U.S.A.* 101 (27), 9971–9975.
- Pipolo E., A., Sinclair, T.S., Camara, G.M.S., 2004. Effects of temperature on oil and protein concentration in soybean seeds cultured in vitro. *Ann. Appl. Biol.* 144, 71–76.
- Qiu, Y., Jiang, Y., Guo, L., Burkey, K., Zobel, R.W., Shew, H.D., Hu, S., 2018. Contrasting warming and ozone effects on denitrifiers dominate soil N₂O emissions. *Environ. Sci. Technol.* 52, 10956–10966.
- R Core Team, 2019. R: A language and environment for statistical computing. R Foundation for Statistical Computing, Vienna, Austria. URL (<https://www.R-project.org/>).
- Rashid, M., Andersen, M., Wollenweber, B., 2018. Impact of heat-wave at high and low VPD on photosynthetic components of wheat and their recovery. *Environ. Exp. Bot.* 147, 138–146.
- Rogers, A., Humphries, S.W., 2000. A mechanistic evaluation of photosynthetic acclimation at elevated. *Glob. Change Biol.* 6 (1005–1011), CO₂-1011. <https://doi.org/10.1046/j.1365-2486.2000.00375.x>.
- Rosenthal, D., Ruiz-Vera, U.M., Siebers, M.H., Gray, S.B., Bernacchi, C.J., Ort, D.R., 2014. Biochemical acclimation, stomatal limitation and precipitation patterns underlie decreases in photosynthetic stimulation of soybean (*Glycine max*) at elevated [CO₂] and temperatures under fully open air field conditions. *Plant Sci.* 226, 136–146.
- Rotundo, L., Westgate, M.E., 2009. Meta-analysis of environmental effects on soybean seed composition. *Field Crops Res.* 110, 147–156.
- Ruiz-Vera, U.M., Siebers, M., Gray, S.B., Drag, D.W., Rosenthal, D., Kimball, M., Ort, B. A., Bernacchi, C.J. R., D., 2013. Global warming can negate the expected CO₂ stimulation in photosynthesis and productivity for soybean grown in the Midwestern United States. *Plant Physiol.* 162, 410–423.
- Saitoh, K., Sugimoto, M., Shidmoda, H., 1998. Effects of dark respiration on dry matter production of field grown rice stand. *Plant Prod. Sci.* 1 (2), 106–112.
- Salem, M., Kakani, V., Koti, S., Reddy, K.R., 2007. Screening of soybean genotypes for high temperatures. *Crop Sci.* 47 (1), 219–231.
- Salvucci, M.E., Crafts-Brandner, S.J., 2004. Inhibition of photosynthesis by heat stress: the activation state of Rubisco as a limiting factor in photosynthesis. *Physiol. Plant.* 120 (2), 179–186. <https://doi.org/10.1111/j.0031-9317.2004.0173.x>.
- Sharkey, T., Bernacchi, C., Farquhar, G.D., Singaas, E.L., 2007. Fitting photosynthetic carbon dioxide response curves for C3 leaves. *Plant Cell Environ.* 30, 1035–1040. <https://doi.org/10.1111/j.1365-3040.2007.01710.x>.
- Shrestha, A., Song, X., Barbour, M.M., 2019. The temperature response of mesophyll conductance, and its component conductances, varies between species and genotypes. *Photosynth. Res.* 141, 65–82.
- Siebers, M.H., Yendrek, C.R., Drag, D., Locke, A.M., Acosta, L.R., Leakey, A.D.B., Ort, D. R., 2015. Heat waves imposed during early pod development in soybean (*Glycine max*) cause significant yield loss despite a rapid recovery from oxidative stress. *Glob. Change Biol.* 21, 3114–3125.
- Tan, K.Y., Zhou, G.S., Ren, S.X., 2013. Response of leaf dark respiration of winter wheat to changes in CO₂ concentration and temperature. *Chin. Sci. Bull.* 58, 1795–1800. <https://doi.org/10.1007/s11434-012-5605-1>.
- Thomey, M.L., Slaterry, R.A., Kohler, I.H., Bernacchi, C.J., Ort, D.R., 2019. Yield response of field-grown soybean exposed to heat waves under current and elevated [CO₂]. *Glob. Change Biol.* 25, 4352–4368.
- Tomeo, N., Rosenthal, D., 2017. Variable mesophyll conductance among soybean cultivars sets a tradeoff between photosynthesis and water-use-efficiency. *Plant Physiol.* 174, 241–527. <https://doi.org/10.1104/pp.16.01940>.
- United States Department of Agriculture. USDA National Agricultural Statistical Service. (2020, October 13). (https://www.nass.usda.gov/Statistics_by_Subject/index.php?setor=CROPS).
- Venables, W.N., Ripley, B.D., 2002. *Modern Applied Statistics with S*, Fourth ed. Springer, New York. ISBN 0-387-95457-0. (<https://www.stats.ox.ac.uk/pub/MASS4/>).
- Watanabe, I., Nagasawa, T., 1990. Appearance and chemical composition of soybean seeds in germplasm collection of Japan. 2. Correlation among protein, lipid, and carbohydrate percentage. *Jpn. J. Crop. Sci.* 59, 661–666.
- Wijewardana, C., Reddy, K., Bellaloui, N., 2019. Soybean seed physiology, quality, and chemical composition under soil moisture stress. *Food Chem.* 278, 92–100. <https://doi.org/10.1016/j.foodchem.2018.11.035>.
- Xu, G., Singh, S., Barnaby, J., Buyer, J., Reddy, V., Sicher, R., 2016. Effects of growth temperature and carbon dioxide enrichment on soybean seed components at different stages of development. *Plant Physiol. Biochem.* 108, 313–322.
- Zhang, Z., Mai, Y., 2018. WebPower: Basic and advanced Statistical Power Analysis. R package version 0.5.2. (<https://CRAN.R-project.org/package=WebPower>).
- Zhao, C., Liu, B., Piao, S., Wang, X., Lobell, D.B., Huang, Y., Huang, M., Yao, Y., Bassu, S., Ciais, P., Durand, J.L., Elliott, J., Ewert, F., Janssens, I.A., Li, T., Lin, E., Liu, Q., Martre, P., Müller, C., Peng, S., Peñuelas, J., Ruane, A.C., Wallach, D., Wang, T., Wu, D., Liu, Z., Zhu, Y., Zhu, Z., Asseng, S., 2017. Temperature increase reduces global yields of major crops in four independent estimates. *Proc. Natl. Acad. Sci. U.S.A.* 114 (35), 9326–9331. <https://doi.org/10.1073/pnas.1701762114>.
- Zheng, H., Chen, L., Han, X., 2009. Response of soybean yield to daytime temperature change during seed filling: a long-term field study in northeast China. *Plant Prod. Sci.* 12 (4), 526–532.